Research progress of gaseous polycyclic aromatic hydrocarbons purification by adsorption

Xiong Yang [1,2], Ziyi Li[1,2,*], Yingshu Liu [1,2,*], Yi Xing[1,2], Jinchao Wei[3], Bentao Yang[3], Chuanzhao zhang[4], Ralph T Yang[5], Chuen-Jinn Tsai[6]

[1] School of Energy and Environmental Engineering, University of Science and Technology Beijing, Beijing, 100083, China

[2] Beijing Higher Institution Engineering Research Center of Energy Conservation and Environmental Protection, Beijing, 100083, China;

[3] Zhongye Changtian International Engineering Co., Ltd., Changsha, 410205, China;

[4] College of Biochemical Engineering, Beijing Union University, Beijing 100023, People's Republic of China;

[5] Department of Chemical Engineering, University of Michigan, Ann Arbor, MI 48109, USA;

[6] Institute of Environmental Engineering, National Chiao Tung University, University Road, Hsinchu 30010, Taiwan

Corresponding authors.

Tel.:+861062334210

Email address: ziyili@ustb.edu.cn(Ziyi Li), ysliu@ustb.edu.cn(Yingshu Liu);

Abstract

Gaseous polycyclic aromatic hydrocarbons (PAHs) are carcinogenic and mutagenic pollutants and also able to promote the growth of secondary particulate matters, which have attracted great attention in recent years. Control of PAHs emissions in exhaust gases using different techniques has been hot topics in the atmospheric environment field. Adsorption is one of the most effective ones and is well accepted by industries in gaseous pollutant removal in which the adsorbent characteristics play critical roles. In this paper, the latest advances in the field of PAHs adsorption are critically reviewed with special emphasis on adsorption-desorption characteristics and related applications. Studies on adsorption equilibrium, kinetics, and desorption properties of PAHs as special low-volatile gases on conventional activated carbons and novel mesoporous adsorbents are summarized and compared, showing the advantages of mesoporous adsorbents over traditional adsorbents in terms of the fast adsorption and facile desorption. The significant factors on the optimal balance between adsorption and desorption as well as the corresponding adsorbent materials are discussed in detail. This work can be a reference for further studies on adsorptive purifications of PAHs and other low-volatile gases.

Keywords: Polycyclic Aromatic Hydrocarbons; Low Volatility; Adsorption; Desorption; Adsorbents.

INTRODUCTION

Polycyclic aromatic hydrocarbons (PAHs, also polyaromatic hydrocarbons or polynuclear aromatic hydrocarbons) are hydrocarbons—organic compounds containing only carbon and hydrogen—that are composed of multiple aromatic rings (organic rings in which the electrons are delocalized). They are the earliest discovered and most abundant types of carcinogens (Villemin *et al*.,1994). PAHs have characteristics of high boiling point, large molecular weight and low vapor pressure. The number of aromatic rings and molecular weight are important factors affecting their physical and chemical properties. Most of the PAHs that have been discovered so far are highly toxic, and some PAHs metabolites or derivatives are potential mutagens(Dat et al., 2018). In 1976, the EPA's list of 129 “priority pollutants” included 16 kinds of PAHs compounds(Keith and Telliard, 1979).

Sources of PAHs mainly include natural sources and man-made sources. Natural effects such as forest fires, volcanic eruptions, and biosynthesis produce small amounts of PAHs(Sugiyama et al., 2017), while with the rapid development of human production and life, man-made sources contribute to greater amounts of PAHs emissions including: (1) incomplete combustion or reduction of various fossil fuels (such as petroleum, coal) and other hydrocarbons; (2) chemical industry, organic chemical raw material industry, chemical raw material manufacturing and other industries; (3) coking industrial production enterprises coking, petroleum cracking, coal tar refining and other processes; (4) trash and waste incinerators(Wang *et al.* 2002, 2009). There is

75 an increasing concern about the occurrence of PAHs as carcinogens, mutagens, teratogens and
76 bioaccumulation since they are ubiquitous in ambient air, airborne particulate matter(Lovet et al.,
77 2018; Zhang et al., 2018) and have great damage on environmental and human beings (Cheng et
78 al., 2004; Yang *et al*., 2008 ; Owabor *et al*., 2010; Long *et al*., 2017).

79 Controlling PAHs emissions has become a hot topic in the field of atmospheric environment
80 research. Previous researches on purifying gaseous PAHs can be classified into two types, the
81 destructive technologies such as photocatalytic degradation(Zhang *et al*., 2008), plasma(Yu *et al.*,
82 2010) and catalytic oxidation(Shie *et al.*, 2005), and the recoverable technologies such as
83 adsorption, absorption, condensation and membrane separation. Among them, adsorption is
84 considered to be one of the most promising PAHs purification methods because of its cost-
85 effectiveness, simple operation and high removal efficiency at low concentrations(Ghafari and
86 Atkinson, 2018; Tseng et al., 2002; Liu et al., 2002; McKay et al., 2002). The characteristics of
87 adsorbents and an appropriate selection of the materials play critical roles in practical use of
88 adsorption purification technologies. The high adsorption capacity, fast adsorption rate and low
89 regeneration energy consumption are commonly the targeted characteristics that an ideal
90 adsorbent should process.

91 In comparison to ordinary gases, gaseous PAHs with larger molecular weights and low
92 volatilities render different adsorption characteristics, for instance, the stronger affinity on the

pore surfaces and thus the significant adsorption capacity at very low concentrations. However, the larger molecular sizes of PAHs are not conducive to adsorption diffusion and mass transfer inside the pores of adsorbents, and therefore greatly reduce the adsorption rate. Besides, due to the strong interactions between PAHs and adsorbents, a much higher thermal desorption temperature for adsorbent regeneration would be required, which causes higher energy consumption in temperature swing adsorption processes in practical applications. Therefore, the exploration of the optimal balance between PAHs adsorption and desorption has become one of the core research content of PAHs adsorption purification. Activated carbons as a type of adsorbents are widely accepted in industry due to the low price and great PAHs adsorption capacity, and need high desorption temperatures and higher regeneration energy consumption due to the rich microporosity. With the rapid development of mesoporous materials in recent years, adsorptive removal of PAHs based on ordered mesoporous adsorbents has gradually entered scholar's vision, which could be a replacement for activated carbons and has potentials of solving corresponding practical problems. Mesoporous materials not only have large and ordered mesopores to promote adsorption and desorption mass transfer, but remain satisfactory adsorption capacity of PAHs at low concentrations regarding the coexisting micropores. This paper focuses on introductions, comparisons and evaluations of various PAHs adsorbents and related

characteristics, and proposes a prospect for the development of PAHs adsorption purification technology.

BASIC PHYSICAL PROPERTIES AND CHEMICAL STRUCTURE OF PAHS

PAHs are hydrocarbons—organic compounds containing only carbon and hydrogen, that are composed of multiple aromatic rings. Most of them have relatively high molecular symmetries. The Chemical structures of the 16 United States Environmental Protection Agency (USEPA) priority PAH compounds is shown in Fig. 1(Okparanma and Mouazen, 2013). The characteristic of 16 USEPA priority PAHs are summarized in table 1. They have molecular mass ranging from 128g mol^{-1} for naphthalene to 278 g mol^{-1} for dibenzo[a,h]anthracene. Their boiling point increase with the increasing of the formula weight and ranging from 218 ℃ for naphthalene to 542 ℃ for benzo[g,h,i]perylene. The solubility, sorption, and vapour pressure for each PAH are important factors that determine the proportion in the environment (Huang et al., 2003). Low molecular weight or 2–3 rings PAHs usually found in gas-phase PAH concentrations, whilst those with four or more rings are found most in particle phase(Liu et al., 2017). PAHs are also known to exhibit very low water solubilities and hydrophobicities.

PAHs have been linked to skin, lung, bladder, liver, and stomach cancers in well-established animal model studies. As they have different chemical structure, the PAHs show a different

toxicity and damage to human body. They can damage human body through inhalation, skin and eyes contact, drink and eating. The carcinogenicity of PAHs increases with increasing the increasing of formula weight. Their toxicity and preventive measures are also list simply in Tab. 1.

ADSORPTION CHARACTERISTIC OF PAHS

Adsorption equilibrium of PAHs

The study on adsorption equilibrium of PAHs mainly involves the adsorption isotherm model and the equilibrium adsorption capacity.

Adsorption on active carbon

Because of high specific surface area(ranging from 300 m^2/g to 3000 m^2/g) (Lamichhane, 2016) and low price, activated carbon is being a very popular in removal of pollution component, such as mercury(Tsai et al., 2017), formaldehyde(Shiue et al.,2018), SO_2(Liu et al., 2019), and also PAHs (Lamichhane, 2016).

Mastral et al.(2001a) obtained adsorption equilibrium parameters of PAHs on 16 different activated carbons, including asphalt-based, coal-based, apricot-based, cherry-based, grape-based, and coconut-shell activated carbons. On the basis of quasi-equilibrium adsorption tests for three PAHs (2-4 rings), naphthalene, phenanthrene, and pyrene, the narrow micropores (pore size < 0.7 nm) were found to be more favorable for naphthalene adsorption, while the adsorption of

150 phenanthrene is more dependent on the total pore volume and micropore distribution, and the
151 adsorption of pyrene is directly related to the total volume of mesopores (2−50 nm). The
152 difference in the pore size distributions between above carbon materials has a greater impact on
153 PAHs adsorption as compared to the difference in surface functional groups. It is therefore
154 judged that the textural characteristics of the adsorbent are dominant factors in PAHs adsorption.
155 Ravenni et al.(2018) summarized the adsorption capacity of ACs on PAHs was mostly dependent
156 on their porous-textural characteristics, especially microporosity.

157 In terms of the adsorbate, the work done by Mastral et al.(2003) extended to 7 PAHs and their
158 adsorption isotherms on a certain coke at concentrations ranging from 0.020 to 25 ppm and the
159 temperature of 150 °C. The Langmuir and Freundlich models were found to describe the
160 adsorption equilibrium of these PAHs well, the former one being suitable for naphthalene
161 corresponding to either uniform and monolayer adsorption or microporous filling effect, and the
162 latter one being suitable for phenanthrene, acenaphthene, and anthracene, etc. corresponding to
163 non-uniform adsorption and multilayer adsorption. Ma et al.(2004) compared the PAHs
164 adsorption on 6 adsorbents at conditions of flue gases, and obtained similar conclusions from
165 Mastral et al. (2003), that is, the positive correlation of adsorption effect with the adsorbent's
166 specific surface area and micropore volume. Zhou et al.(2010a) investigated the adsorption
167 equilibrium of naphthalene on three activated carbons and pointed out the significant difference

between granular and powder activated carbons exhibiting monolayer adsorption described by the Langmuir model and multilayer adsorption described by the BET model, respectively. Di Gregorio et al.(2016) investigated the removeal of naphthalene(reference tar compound) by active carbons at(750°C to 900°C), the results shows active carbon could reach a removal efficiencies of above 90%, and adsorption contributed more than 90% of the removal efficiency.

Tab. 2 lists the equilibrium adsorption capacity of each adsorbate-adsorbent pair mentioned above. It's worth noting that the adsorption temperature of gaseous PAHs in the reference is generally set at 125-160℃. This is because the study of gaseous PAHs adsorption is mainly directed to flue gas. For brief presentations and convenient comparisons, the similar equilibrium concentrations and the adsorbents giving higher adsorption capacities from different literatures are selected. It can be observed that for different PAHs, the variation rules of the adsorption capacity on different adsorbents are similar. The apricot-based and coal-based activated carbons with wider pore size distributions and larger average micropore diameters have higher PAHs adsorption capacities(Mastral et al., 2002a) probably attributed to the greater adsorption diffusion characteristics for macromolecular PAHs, which further demonstrates that physical textural properties play vital roles. For the same adsorbent, the PAHs adsorption capacity increases with increasing molecular weight or ring number, indicative of the increasing adsorption strength with the decrease in volatility.

Adsorption on mesoporous materials

187 Typical mesoporous adsorbents have showed a high adsorption capacity on VOCs adsorption
188 for their tailorable pore system(Zeng and Bai, 2016). They have been commonly used for
189 studying PAHs adsorption include ordered mesoporous silica MCM-41and SBA-15, and ordered
190 mesoporous carbon CMK-3, CMK-5 (reversed structure of SBA-15 as the hard template in
191 synthesis) and FDU-15 (micro-mesopore coexisting structure). Figure 2 shows the structure
192 diagrams of MCM-41, SBA-15 and CMK-3. MCM-41 is featured with unconnected and regular
193 mesopores as one-dimensional (1D) channels(Beck et al., 1992), while SBA-15 has
194 complementary micropores and small mesopores in the silica walls connecting the primary 1D
195 mesopore channels forming a 2D hexagonal array(Kosuge et al., 2007; Zhao et al., 1998). As a
196 negative replica structure of SBA-15(Vinu et al., 2006), CMK-3 can be described as a network of
197 carbon rods with ordered mesopores in between and micropores in the walls of the
198 nanorods(Ryoo et al., 1999).
199 Wang et al.(2012,2013) synthesized ordered mesoporous carbons (OMCs) with the soft
200 template method and studied the naphthalene adsorption on them. The results showed that the
201 Langmuir model fitted the naphthalene adsorption equilibrium on OMC with the pore size
202 ranging from 2 to 3.5 nm, showing a large adsorption affinity for naphthalene with the adsorption
203 capacity as high as 1.76 mol kg^{-1} at the temperature of 120 °C and the equilibrium concentration
204 of 0.006 mol m^{-3}. The works of Li, et al.(2017b), Yang et al.(2015), and Liu et al.(2016) studied

the adsorption equilibrium of naphthalene, phenanthrene and pyrene on MCM-41, SBA-15 and CMK-3, respectively, demonstrating that sufficient micropores are the key factors in PAHs adsorption enhancement, and the importance of the mesoporous pore volume and pore size distribution grows with increasing PAH molecular weight. Naphthalene was subject to monolayer adsorption with distinct micropore filling pattern on CMK-3, while phenanthrene and pyrene with less micropore filling effect showed non-uniform adsorption states contributed by affinities from both micropores and mesopores. The Langmuir and Freundlich models are suitable for describing the adsorption equilibrium of PAHs with lower (naphthalene) and higher (pyrene) molecular weights, respectively. For phenanthrene with intermediate molecular weight, the Freundlich model performs better on SBA-15 while the Langmuir model performs better on MCM-41 and CMK-3. Meng et al.(2017) compared the adsorption equilibrium of naphthalene on CMK-3, CMK-5 and FDU-15, showing the good isotherm correlations with Langmuir and Sips models and the naphthalene adsorption capacity order of CMK-5 > CMK-3 > FDU-15. CMK-3, CMK-5 and FDU-15 are suitable for naphthalene adsorption at high concentrations, medium and low concentrations, and low concentrations, respectively.

For predicting the phase equilibrium of adsorption, Grand Canonical Monte Carlo method simulation is become a common techniques (Fan et al., 2017; Wang et al.,2018; Yang et al.,2019). Wang et al.(2018) use Grand Canonical Monte method to simulate the naphthalene adsorption

223 behavior in OMC, the results showed the adsorption isotherm curve is of the Langmuir IV type,
224 the maximum capacity reached 105.4 mg g^{-1}. Yang et al.(2019) use Grand Canonical Monte
225 method to simulate naphthalene, phenanthrene, and pyrene adsorption behavior on MCM-41, the
226 results showed the adsorption isotherm curve is belonged to Type I according to the IUPIC
227 classification. And the adsorption capacity follows Pyr > Phe > Nap, the area of the π-electron
228 plane on the PAHs increases with the increasing ring number lead to stronger adsorption
229 interactions.

230 The adsorption equilibrium data for PAHs on mesoporous adsorbents in literatures are also
231 summarized in Tab. 2. It can be seen that MCM-41 containing only mesopores has lower
232 adsorption capacities of PAHs. The mesoporous materials with micro-mesoporous coexisting
233 structures have higher PAHs adsorption capacities at lower equilibrium concentrations, even
234 higher than some conventional activated carbons, indicating the significant role of microporosity
235 regarding PAHs adsorption at low concentrations. When the ring number of PAHs increases, the
236 effects of mesopores become more significant and therefore mesoporous materials give higher
237 adsorption capacities for high-ring PAHs.

238 ***Adsorption kinetics of PAHs***

239 The adsorption kinetics is another significant property for PAHs adsorbent in terms of the rates
240 of adsorption and desorption, of which the studies mainly deal with the kinetic model fitting to
241 experimental data of adsorption breakthrough curves. Afterwards, the internal, external and

overall adsorption mass transfer coefficients can be obtained. Take the linear driving force (LDF) model as an example to introduce the three mass transfer coefficients(Li and Yang, 1999; Todd and Webley,2002; Li et al., 2018), which follows the expressions as:

$$\frac{\partial q}{\partial t} = k_p(q_s - q) \tag{1}$$

Where The term $\partial q/\partial t$ represents the local adsorption rate, k_p is the internal mass-transfer coefficient in the stationary phase (s^{-1}); q_s is the concentration adsorbed at adsorbent surface (mol kg^{-1});

There are two other common expressions for the local adsorption rate in terms of the external and internal mass-transfer coefficients as:

$$\rho\frac{\partial \overline{q}}{\partial t} = k_f\alpha(C - C_s) \tag{2}$$

$$\rho\frac{\partial \overline{q}}{\partial t} = k_L\alpha(C - C^*) \tag{3}$$

where α is the mass-transfer area per unit volume of the bed; C is the gas concentration at the main liquid (mol m^{-3}); C_s is the gas concentration at the adsorbent exterior surface (mol m^{-3}); k_f is the external mass-transfer coefficient across the gas film on the exterior surface of adsorbents (m s^{-1}); K_L is the overall liquid-phase mass-transfer coefficient (m s^{-1}), and $K_L\alpha$ is called the volumetric mass-transfer coefficients (s^{-1}); C* is the gas phase concentration in equilibrium with the solid phase concentration q* (mol m^{-3}), in the adsorption isotherm relationship expressed by q* = f(C*). The relationship between the overall mass-transfer coefficient and the individual mass-transfer coefficients could be given by:

$$\frac{1}{k_L\alpha}=\frac{1}{k_f\alpha}+\frac{C_0}{k_p\rho q_0} \quad (4)$$

For the studies on conventional adsorbents, Murillo et al. (2004) used the simplified LDF mass transfer model to obtain the adsorption kinetics, providing k_p of phenanthrene on three activated carbon materials ranging from 1×10^{-3} to 2×10^{-3} s^{-1} at an equilibrium concentration of 0.001 mol m^{-3}. Mei et al.(2014) studied the adsorption kinetics of naphthalene on activated carbons at different temperatures and flow rates with a fixed-bed test and numerical prediction by the Yoon-Nelson mass transfer zone model giving the length and the moving of the mass transfer zone throughout the bed.

For adsorption kinetics of macromolecular PAHs on ordered mesoporous adsorbents, the advantages that are shown below have attracted attention. Yang et al.(2015) found that SBA-15 had higher adsorption rate for naphthalene due to the presence of micro-meso cross-linked pore structure, compared to MCM-41 with a 1-D mesopore structure. Liu et al.(2016) established an adsorption breakthrough curve model based on the constant concentration wave hypothesis, and explored the adsorption kinetics of naphthalene on three mesoporous adsorbents. The results indicated that internal diffusion was the main rate-control step for the adsorption and mass transfer of PAHs on mesoporous materials. The mesoporous structure can effectively reduce the internal diffusion resistance and improve the overall mass transfer coefficient. Li et al.(2017a) studied the adsorption and kinetics of phenanthrene on mesoporous silicas and carbon, showing

275 that the large primary mesopore size and the cross-linked pore structure rich in micropores and
276 fine mesopores contribute a lot to phenanthrene adsorption mass transfer. Based on three
277 mesoporous carbon materials, Meng et al.(2017) further proved the important role of the micro-
278 meso cross-linked pore structure in improving PAHs adsorption mass transfer, where the
279 advantage of CMK-5 stands out.

280 Tab. 3 summarizes the adsorption kinetic parameters of naphthalene, phenanthrene and pyrene
281 in three typical mesoporous adsorbents from literatures. As can be seen from the table, when the
282 concentration is low and the PAHs molecular weight is small, the overall adsorption mass
283 transfer rate follows CMK -3 > SBA-15 > MCM-41. When the concentration is higher and the
284 molecular weight of the adsorbate is larger, the overall adsorption mass transfer rate follows SBA
285 -15 > CMK-3> MCM-41. Compared to traditional activated carbons, k_p on the mesoporous
286 material is higher at similar equilibrium concentrations indicating the small internal diffusion
287 resistance and the greater mass transfer advantage which increases with increasing PAHs'
288 molecules size. For the adsorption of small molecular naphthalene, the microporous filling on
289 CMK-3 and the hydrophobicity of the carbon-based surface are obvious. For the adsorption of
290 larger molecules of phenanthrene and pyrene, the role of mesopores on mass transfer is gradually
291 enhanced. The larger mesopores and micro-meso cross-linked structures of SBA-15 exhibit
292 significant diffusion advantages. CMK-3 exhibits higher mass transfer coefficients due to its

larger mesopore volume. The one-dimensional smaller mesopores on MCM-41 gives simple adsorption diffusion behavior of PAHs and irregular variation of the diffusion coefficient with increasing concentration when the adsorbate's molecular size increases.

PAHs adsorption influential factors

Effect of surface functional groups

The PAHs are uncharged and non-polar molecules molecule with planar ring structures. Many studies have shown that the difference in surface functional groups of the adsorbent has little effect on PAHs adsorption, especially for those with higher symmetries such as naphthalene and pyrene. Mastral et al.(2001b) showed that the main factor influencing PAHs adsorption is not the active site on the adsorbent, but the physical properties of the pore size distribution and the pore structure(2002b). The result shows PAH adsorption capacities on carbons is positively correlated with pore volume. Some work showed that reducing the original oxygen-containing functional groups of activated carbons can effectively increase the adsorption capacity of phenanthrene, and the presence of oxygen surface groups (i.e., both CO and CO_2-type groups) can lead to a decrease in phenanthrene adsorption capacity(2004). This is because the adsorption of phenanthrene will involve the interaction of the electron-rich regions located in graphene layers with the π electrons of the aromatic compounds. The increasing of the oxygen groups on active carbon results in electron withdrawal from the graphene layers (π–π argument), and consequently decreases the specific interaction between phenanthrene and the carbon surface. Considering that the cyclic

molecules of PAHs may exhibit the π-electron interaction with the surface graphene ring, it is believed that the adsorption of PAHs is mainly subject to physical adsorption with potentially weak chemical interactions. Mastral et al.(2004) claimed that for active carbons the critical preferential physical factors for PAHs adsorption include the appropriate pore size with diameter approximately twice the PAH molecular size besides the highly developed porosity.

Effect of CO_2

CO_2 is a common component in flue gases, which is easy to form competitive adsorption with trace amounts of PAHs on adsorbents. Mastral et al.(2002c) found there exists a negative influence of CO_2 on phenanthrene adsorption as shown in Figure 3. The figure gives different adsorption isotherms of phenanthrene on a carbonaceous material at different CO_2 concentrations, and shows that 15% of CO_2 decreases phenanthrene adsorption capacity by 24%. However, the negative influence of CO_2 fails to increase significantly with CO_2 concentrations, as evidenced by the nearly unchanged phenanthrene adsorption capacity when CO_2 concentration increases from 10% to 30%,. It can be judged that a robust PAHs adsorbent should possess a wide pore size distribution and a higher average micropore diameter which are helpful to inhibit strong competitive adsorption of CO_2. From this perspective, the development of mesoporosity in adsorbents promotes phenanthrene adsorption because it is able to either favor the access of phenanthrene molecules into the micropores to form potentially multilayer adsorption or weaken CO_2 competitive adsorption.

Effect of moisture

Influences of moisture on phenanthrene adsorption on 16 carbonaceous materials was once studied by Mastral et al.(2002d). The influence was largely associated with the microporosity of the adsorbent. The effect of moisture on Phe adsorption was positively correlated with the narrow micropore volume (pore size diameter < 0.7 nm) with a statistical significance level higher than 99%. This is probably due to the fact that at low humidity partial pressures, the water molecules are retained mainly in the molecular size micropores (ca. 0.3 nm). Therefore, the higher the narrow microporosity is, the higher the water adsorption and the lower the Phe adsorption.

DESORPTION PROPERTIES OF PAHS

The desorption characteristics is highly related to the cyclic performance of the adsorbent as well as the energy consumption during actual operation which is a big challenge to practical applications, particularly for the low-volatility PAHs at low concentrations. The most widely used method for obtaining desorption information is based on thermogravimetric analysis (TGA), in which temperature-programmed desorption (TPD) is recorded under any heating profile.(Park and Yang 2005; Adelodun et al., 2016) The key kinetic information (or, "kinetic triplet")—the activation energy, the pre-exponential factor, and the kinetic model—can be determined with combined kinetic analysis of experimental data.(Perez-Maqueda et al., 2002) According to this line of research, previous studies have dealt with the adsorbents for desorption of organic pollutants, such as dibenzo-p-furane on zeolites(Xi et al., 2003). The peak desorption and the desorption

activation energy are two key parameters that have been studied in research of PAHs desorption properties.

Li et al.(2016) investigated desorption performances of naphthalene and pyrene on mesoporous MCM-41, SBA-15, and CMK-3 at the temperature of 350–800 K and different heating rates based on temperature-programmed desorption (TPD) experiments, and obtained the desorption activation energy, pre-exponential factor, and kinetic model for each adsorbate–adsorbent pair with a combined model-fitting method. The results showed SBA-15 with interconnectivity between adjacent mesopores offered diffusion advantages in desorption, which contributes to the order of the degree of ease in desorption: SBA-15 > MCM-41 > CMK-3. Subsequently, the desorption kinetics of naphthalene and anthracene on two activated carbons were also studied by a similar method(Li *et al.*, 2015). The Johnson–Mehl–Avrami (JMA) rate equation following the nucleation and growth model was found to best describe the PAH desorption from both adsorbents, showing significant molecular sieving effects on desorption characteristics. The active carbons with less narrow micropore (<0.7 nm) volume and more wide micropores (0.7–2 nm) favor PAH adsorption and desorption rates. Zhou et al.(2010b) used the main curve method to study the desorption kinetics of naphthalene and acenaphthene on activated carbons, and pointed out that the mechanism of desorption rate is correlated with the JMA equation. The average desorption activation energies of naphthalene and acenaphthene calculated by the iso-conversional method are 65.89 and 96.13 kJ mol^{-1}, respectively. Guilloteau et al.(2008,2009) studied the desorption characteristics of 3-5 ring PAHs on laboratory-generated kerosene soot surfaces, and obtained the Arrhenius expression based on analysis of the desorption rate constant and desorption activation energy. Su et al.(2010) worked on the adsorption and desorption properties of C2-C12 VOCs on MCM-48, and found that the mesoporosity was able to effectively reduce the desorption temperature (100-180°C) compared with conventional carbon materials.

The facile desorption was accompanied by a low memory effect, since the large mesopores of MCM-48 could be regenerated more efficiently during thermal desorption.

Tab. 4 summarizes the TPD peak temperatures and the desorption activation energies of PAHs on conventional activated carbons and mesoporous adsorbents. It can be clearly seen that the desorption temperatures of PAHs on mesoporous adsorbents are lower than those on activated carbons, indicating the promoted macromolecular diffusion and mass transfer characteristics by mesopores. For the desorption activation energy, SBA-15 and CMK-3 with co-existing micropores and mesopores also give lower values as compared to activated carbons, largely attributed to their special micro-meso cross-linked pore structures. However, MCM-41 with one-dimensional mesoporosity fails to show significant advantages of desorption over activated carbons. Tab. 4 also shows the TPD peak temperatures and desorption activation energies of PAHs on the same adsorbent increase with the increasing of the molecular weight. It is indicated the energy required for desorption of PAHs from adsorbent increases with the increase of molecules. This is because the PAHs with higher molecular weight have stronger adsorption interactions due to larger π-electron plane area on the PAHs. This is consistent with the adsorption capacity of PAHs on adsorbent.

APPLICATION RESEARCHES OF PAHS ADSORPTION PURIFICATION

Current researches on practical applications of PAHs adsorption primarily involve flue gas purification, cigarette filtration, and sampling and detection. With the increasing strict environmental protection standards in recent years, the application researches on PAHs adsorption purification from flue gases has been increasing, where traditional activated carbons

400 are widely accepted mainly due to the cheapness. Mesoporous adsorbents with relatively higher
401 prices are mainly used in cigarette filtration and small-scale atmospheric sampling and detection.
402 For the PAHs purification in flue gases, Aranda et al.(2007) used the temperature swing
403 adsorption technology with activated carbons to study the adsorptive removal of typical PAHs in
404 the hot flue gas. The results showed that the adsorption performance largely depended on
405 adsorbent characteristics such as total micropore volume and micropore size distribution. It was
406 found that the adsorption capacity of naphthalene remained unchanged with adsorption cycling,
407 while that of phenanthrene dropped sharply after the first run and is stabilized afterwards. Mastral
408 et al. (2001c) added limestone mixed with pulverized coal in a circulating fluidized combustion
409 bed for PAHs removal in flue gases, and found that it can reduce the emissions of gaseous PAHs
410 as well as the conversion to particulate matters. Zhong et al.(2008) presented the research of
411 PAHs adsorption purification in municipal solid wastes (MSW) incineration with in-pipe jet
412 adsorption techniques, showed the increasing removal effectiveness with increasing injection
413 weight of adsorbents, and gave the order of adsorbent performance in PAHs purification of
414 kaolin > activated carbon > activated bauxite. Zhou et al.(2005) studied the effect of pipe-sprayed
415 activated carbons on the removal of PAHs from the municipal solid waste flue gas, and showed
416 appealing removal efficiencies of PAHs ranging from 76% to 91%. With the increase of the

adsorbent feeding rate, the concentrations of three- to six-ring PAHs in fly ash increased, and those of two-ring PAHs decreased.

For other application researches of PAHs, Meier and Siegmann (1999) added 4% of NaY to the cigarette to reduce PAHs and nitrosamines, showed significant reductions of PAHs in the smoke with an efficiency of 43±9 %. Zhou et al(2004,2008) demonstrated that Y zeolite had a better PAHs adsorption performance compared to ZSM-5 in purifying the cigarette smoke. The NaY zeolite coated with CuO significantly enhanced the PAHs removal efficiency with the optimal condition of 3% CuO/NaY. This novel material with nano-pore structures can effectively reduce 30%-60% of harmful contents like PAHs and nitrosamines in cigarette smoke. Yong et al.(2006) studied the adsorption characteristics of PAHs in cigarette smoke with MCM-48 and Ce-MCM-48, showing that the incorporation of cerium into MCM-48 as mesoporous shape-selective adsorption/catalysts can effectively improve the catalytic activity and PAH removal. Lee et al.(2006) investigated the adsorption properties of 7 semi-volatile PAHs(including acenaphthylene， acenaphthene， fluorene， phenanthrene， anthracene， fluoranthene and pyrene) on a studied the adsorption properties resin XAD-4. The results showed the 4-ring PAHs are more easily adsorbed than the 3-ring PAHs, because the area of the π-electron plane on the PAHs increases with the increasing ring number, lead to stronger adsorption interactions. The

physical behavior of PAHs on XAD-4 might involve an aerosol form rather than a gaseous adsorption.

CONCLUSIONS

(1) The adsorption purification studies of gaseous PAHs focus on the selection of adsorbents and the adsorption and desorption characteristics. Conventional activated carbons have the advantages of low price and high adsorption capacity for PAHs at low concentrations and disadvantages of low adsorption uptake rate and high desorption energy consumption. Mesoporous adsorbents have satisfactory adsorption capacity, higher adsorption rate, more facile desorption and greater sustainability compared to activated carbons. This is because mesoporous adsorbents have high pore volume, larger pore size and micro-meso cross-linked pore structure, it will effectively reduce the internal diffusion resistance and improve the overall mass transfer coefficient on adsorption and desorption.

(2) The adsorption of PAHs is mainly physical adsorption, and a wide pore size distribution is the key factor for a robust PAHs adsorbent. Microporosity is to PAHs adsorption at low concentrations, but too many narrow micropores would lead to mass transfer diffusional troubles and higher desorption temperatures and activation energies. Mesoporosity can promote adsorption and desorption rate, lower the desorption temperature, reduce the negative effects of moisture, CO_2 and other impurity gases on PAHs adsorption.

(3) For mesoporous adsorbents, the regulation of micro-meso cross-linking structure is the key factor to obtain the optimal balance between adsorption and desorption of PAHs. Benefiting from this, SBA-15 and CMK-5 are found to be the preferred silica-based and carbon-based PAHs mesoporous adsorbents, respectively.

ACKNOWLEDGMENTS

This research was suppored by the National Natural Science Foundation of China (51604016, 21676025, 51478083), National Key R&D Program of China (No. 2017YFC0210302), the National Postdoctoral Program for Innovative Talents (No. BX201700029), Beijing Natural Science Foundation (No. 8174064, 8182019), the China Postdoctoral Science Foundation (No. 2018M630075) and the Fundamental Research Funds for the Central Universities (No. FRF-TP-17-063A1, FRF-BD-18-015A).

REFERENCES

Aranda A, Navarro M V, García T, et al. (2007). Temperature swing adsorption of polycyclic aromatic hydrocarbons on activated carbons. Ind. Eng. Chem. Res. 46(24): 8193-8198.

Adelodun, A. A., Ngila, J. C., Kim, D. G., & Jo, Y. M. (2016). Isotherm, thermodynamic and kinetic studies of selective CO2 adsorption on chemically modified carbon surfaces. Aerosol

475 Air Qual. Res, 16(12), 3312-3329.

476 Beck J S, Vartuli J C, Roth W J, et al. (1992).A new family of mesoporous molecular sieves
477 prepared with liquid crystal templates. J. Am. Chem. Soc. 114(27): 10834-10843.

478 Cai H X. (2011).Study on Static and Dynamic Adsorption Behaviors of PAHs in Flue Gas
479 [Dissertation]. Nanjing: Nanjing University of Information Science & Technology,

480 Cheng X, Kan A T, Tomson M B. (2004). Naphthalene adsorption and desorption from aqueous
481 C60 fullerene. J Chem. Eng. Data 49(3): 675-683.

482 Dat N D, Lyu J M, Chang M B.(2018). Variation of Atmospheric PAHs in Northern Taiwan
483 during Winter and Summer Seasons. Aerosol Air Qual. Res., 18(4): 1019-1031.

484 Di Gregorio F, Parrillo F, Salzano E, et al.(2016). Removal of naphthalene by activated carbons
485 from hot gas[J]. Chem. Eng. J., 291: 244-253.

486 Fan F, Zhang M, Peng Z, et al.(2017). Direct simulation Monte Carlo method for acoustic
487 agglomeration under standing wave condition. Aerosol Air Qual. Res., 17(4): 1073-1083.

488 Garcıa T, Murillo R, Cazorla-Amoros D, et al. (2004).Role of the activated carbon surface
489 chemistry in the adsorption of phenanthrene. Carbon 42(8-9): 1683-1689.

490 Ghafari M, Atkinson J D. (2018). Impact of styrenic polymer one-step hyper-cross-linking on
491 volatile organic compound adsorption and desorption performance. J. Hazard. Mater. 351: 117-

123.

Guilloteau A, Bedjanian Y, Nguyen M L, et al.(2009). Desorption of polycyclic aromatic hydrocarbons from a soot surface: three-to five-ring PAHs. J. Phys. Chem. A, 2009, 114(2): 942-948.

Guilloteau A, Nguyen M L, Bedjanian Y, et al. (2008). Desorption of polycyclic aromatic hydrocarbons from soot surface: pyrene and fluoranthene. J. Phys. Chem. A 112(42): 10552-10559.

Huang W, Peng P, Yu Z, et al. (2003). Effects of organic matter heterogeneity on sorption and desorption of organic contaminants by soils and sediments. Appl. Geochem. 18(7): 955-972.

Jin, T., Han, M., Han, K., et al. (2018). Health risk of ambient PM10-bound PAHs at bus stops in spring and autumn in Tianjin, China. Aerosol Air Qual. Res, 18, 1828-1838.

Keith L, Telliard W. (1979). ES&T special report: priority pollutants: Ia perspective view. Environ. Sci. Technol., 13(4): 416-423.

Kosuge K, Kubo S, Kikukawa N, et al. (2007).Effect of pore structure in mesoporous silicas on VOC dynamic adsorption/desorption performance. Langmuir 23(6): 3095-3102.

Lamichhane S, Krishna K C B, Sarukkalige R(2016). Polycyclic aromatic hydrocarbons (PAHs) removal by sorption: a review. Chemosphere, 148: 336-353.

509 Lee J J, Chuang C J.(2006). The characteristics of nano-scale adsorption mechanism on the
510 collection of semi-volatile PAHs with XAD- 4 porous adsorbent[J]. Chin. J. Process Eng.
511 6(s2):150-154.

512 Li Z, Liu Y, Wang H, et al.(2018). A numerical modelling study of SO2 adsorption on activated
513 carbons with new rate equations. Chem. Eng. J., 353: 858-866.

514 Li Z, Liu Y, Yang X, et al. (2015). Desorption kinetics of naphthalene and acenaphthene over
515 two activated carbons via thermogravimetric analysis. Energy Fuels 29(8): 5303-5310.

516 Li Z, Liu Y, Yang X, et al. (2016). Desorption of polycyclic aromatic hydrocarbons on
517 mesoporous sorbents: thermogravimetric experiments and kinetics study. Ind. Eng. Chem. Res.
518 55(5): 1183-1191.

519 Li Z, Liu Y, Yang X, et al. (2017a). Performance of mesoporous silicas and carbon in adsorptive
520 removal of phenanthrene as a typical gaseous polycyclic aromatic hydrocarbon. Micropor.
521 Mesopor. Mat. 239: 9-18.

522 Li Z, Liu Y, Yang X, et al. (2017b). Adsorption thermodynamics and desorption properties of
523 gaseous polycyclic aromatic hydrocarbons on mesoporous adsorbents. Adsorption 23(2-3):
524 361-371.

525 Li Z, Yang R T. (1999). Concentration profile for linear driving force model for diffusion in a

526 particle. AIChE J. 45(1): 196-200.

527 Liu, J., Wang, Y., Li, P. H., et al. (2017). Polycyclic aromatic hydrocarbons (PAHs) at high
528 mountain site in North China: Concentration, source and health risk assessment. Aerosol Air
529 Qual. Res, 17, 2867-2877.

530 Liu S, Yu X, Lin G, et al.(2019). Insights into the Effect of Adsorption-Desorption Cycles on
531 SO2 Removal over an Activated Carbon. Aerosol Air Qual. Res., 19: 411-421.

532 Liu Y, Li Z, Yang X, et al. (2016). Performance of mesoporous silicas (MCM-41 and SBA-15)
533 and carbon (CMK-3) in the removal of gas-phase naphthalene: adsorption capacity, rate and
534 regenerability. RSC Adv. 6(25): 21193-21203.

535 Liu Z S, Wey M Y, Lin C L. (2002). Simultaneous control of acid gases and PAHs using a spray
536 dryer combined with a fabric filter using different additives. J. Hazard. Mater. 91(1-3): 129-
537 141.

538 Long A S, Lemieux C L, Gagné R, et al. (2017).Genetic Toxicity of Complex Mixtures of
539 Polycyclic Aromatic Hydrocarbons: Evaluating Dose-Additivity in a Transgenic Mouse Model.
540 Environ. Sci. Technol. 51(14): 8138-8148.

541 Lovett C, Shirmohammadi F, Sowlat M H, et al.(2018). Commuting in Los Angeles: cancer and
542 non-cancer health risks of roadway, light-rail and subway transit routes. Aerosol Air Qual. Res.,

543 18(9): 2363-2374.

544 Ma Z, Chen H, Li W, et al. (2004). Polycyclic aromatic hydrocarbons removal from hot gas by
545 porous sorbent adsorption. J. Fuel Chem. Technol. 32(5): 526-530.

546 Mastral A M, García T, Callén M S, et al. (2001a). Removal of naphthalene, phenanthrene, and
547 pyrene by sorbents from hot gas. Environ. Sci. Technol. 35(11): 2395-2400.

548 Mastral A M, García T, Callén M S, et al. (2001b).Assessement of phenanthrene removal from
549 hot gas by porous carbons. Energy Fuels 15(1): 1-7.

550 Mastral A M, Garcia T, Callen M S, et al. (2001c). Effects of limestone on polycyclic aromatic
551 hydrocarbon emissions during coal atmospheric fluidized bed combustion. Energy fuels 15(6):
552 1469-1474.

553 Mastral A M, Garcia T, Callen M S, et al. (2002a). Three-ring PAH removal from waste hot gas
554 by sorbents: influence of the sorbent characteristics. Environ. Sci. Technol. 36(8): 1821-1826.

555 Mastral A M, García T, Callén M S, et al. (2002b). Sorbent characteristics influence on the
556 adsorption of PAC: I. PAH adsorption with the same number of rings. Fuel Process. Technol.
557 77: 373-379.

558 Mastral A M, Garcia T, Murillo R, et al. (2002c).Effects of CO2 on the phenanthrene adsorption
559 capacity of carbonaceous materials. Energy Fuels 16(2): 510-516.

560 Mastral A M, Garcia T, Murillo R, et al. (2002d).Moisture effects on the phenanthrene adsorption
561 capacity by carbonaceous materials. Energy Fuels 16(1): 205-210.

562 Mastral A M, García T, Murillo R, et al. (2003). Measurements of polycyclic aromatic
563 hydrocarbon adsorption on activated carbons at very low concentrations. Ind. Eng. Chem. Res.
564 42(1): 155-161.

565 Mastral A M, Garcia T, Murillo R, et al. (2004).Development of efficient adsorbent materials for
566 PAH cleaning from AFBC hot gas. Energy Fuels 18(1): 202-208.

567 McKay G. (2002).Dioxin characterisation, formation and minimisation during municipal solid
568 waste (MSW) incineration. Chem. Eng. J 86(3): 343-368.

569 Mei L, He L, Fan C G, et al. (2014). Adsorption of naphthalene at low concentration on
570 activated carbon. Chin. J. Process Eng. 14 (2) :253-257.

571 Meier W M, Siegmann K. (1999). Significant reduction of carcinogenic compounds in tobacco
572 smoke by the use of zeolite catalysts. Micropor. Mesopor. Mat. 33(1-3): 307-310.

573 Meng M M, Liu Y S, Li Z Y, et al. (2017). Adsorption characteristics of low concentration
574 gaseous naphthalene on ordered mesoporous carbons. CIESC Journal 68 (8) :3109-3118

575 Murillo R, Garcıa T, Aylón E, et al. (2004).Adsorption of phenanthrene on activated carbons:
576 Breakthrough curve modeling. Carbon 42(10): 2009-2017.

577 Okparanma R N, Mouazen A M. (2013). Visible and near-infrared spectroscopy analysis of a
578 polycyclic aromatic hydrocarbon in soils.The Scientific World J.,

579 Owabor, C. N.; Ogbeide, S. E.; Susu, A. A. (2010). Adsorption and desorption kinetics of
580 naphthalene, anthracene, and pyrene in soil matrix. Pet. Sci. Technol. 28, 504

581 Park J H, Yang R T. (2005).Predicting adsorption isotherms of low-volatile compounds by
582 temperature programmed desorption: iodine on carbon. Langmuir 21(11): 5055-5060.

583 Perez-Maqueda, L. A.; Criado, J. M.; Gotor, F. J.; Malek, J. (2002). Advantages of combined
584 kinetic analysis of experimental data obtained under any heating profile. J. Phys. Chem. A
585 106(12): 2862-2868

586 Ravenni G, Sárossy Z, Ahrenfeldt J, et al.(2018). Activity of chars and activated carbons for
587 removal and decomposition of tar model compounds–A review. Renew. Sust. Energ. Rev., 94:
588 1044-1056.

589 Ryoo R, Joo S H, Jun S. (1999).Synthesis of highly ordered carbon molecular sieves via
590 template-mediated structural transformation. J. Phys. Chem. B. 103(37): 7743-7746.

591 Shie J L, Chang C Y, Chen J H, et al. (2005).Catalytic oxidation of naphthalene using a Pt/Al2O3
592 catalyst. Appl. Catal. B-Environ. 58(3-4): 289-297.

593 Shiue A, Hu S C, Tseng C H, et al.(2018). Assessment of Adsorptive Filter for Removal of

Formaldehyde from Indoor Air. Aerosol Air Qual. Res., 18: 3147-3164.

Su Y C, Kao H M, Wang J L. (2010). Mesoporous silicate MCM-48 as an enrichment medium for ambient volatile organic compound analysis. J. Chromatogr. A 1217(36): 5643-5651.

Sugiyama, T., Shimada, K., Miura, K., et al. (2017). Measurement of Ambient PAHs in Kumamoto: Differentiating Local and Transboundary Air Pollution. Aerosol Air Qual. Res, 17, 3106-3118.

Todd R S, Webley P A. (2002). Limitations of the LDF/equimolar counterdiffusion assumption for mass transport within porous adsorbent pellets. Chem. Eng. Sci. 57(19): 4227-4242.

Tsai C Y, Chiu C H, Chuang M W, et al.(2017). Influences of copper (II) chloride impregnation on activated carbon for low-concentration elemental mercury adsorption from simulated coal combustion flue gas. Aerosol Air Qual. Res., 17(6): 1637-1648.

Tseng H H, Wey M Y, Chen J C, et al. (2002).The adsorption of PAHs, BTEX, and heavy metals on surfactant-modified desulfurization sorbents in a dry scrubber. Fuel 81(18): 2407-2416.

Villemin D, Cherqaoui D, Mesbah A.(1994). Predicting carcinogenicity of polycyclic aromatic hydrocarbons from back-propagation neural network. J Chem. Inf. Comp. Sci. 34(6): 1288-1293.

Vinu A, Hossain K Z, Kumar G S, et al. (2006). Adsorption of L-histidine over mesoporous

carbon molecular sieves. Carbon 44(3): 530-536.

Wang K, Huang B, Liu D, et al. (2012). Ordered mesoporous carbons with various pore sizes: Preparation and naphthalene adsorption performance. J. Appl. Polym. Sci. 125(5): 3368-3375.

Wang K, Zhao J, Fu M, et al. (2013). Experimental and molecular simulation study for the preparation of ordered mesoporous carbons. *Aerosol and Air Qual. Res.* 13(3): 1034-1044.

Wang, K., Fu, M., Wu, J., Zhou, G., & Ye, D. (2018). Computer Simulation Studies of Structure Characteristics of Ordered Mesoporous Carbons and its Naphthalene Adsorption Performance. *Aerosol and Air Qual. Res.* 18(2), 542-548.

Wang L C, Lee W J, Tsai P J, et al. (2002). Potential method for reducing emissions of polycyclic aromatic hydrocarbons from the incineration of biological sludge for the terephthalic acid manufacturing industry. Environ. Sci. Technol. 36(15): 3420-3425.

Wang L C, Lin L F, Lai S O. (2009).Emissions of polycyclic aromatic hydrocarbons from fluidized and fixed bed incinerators disposing petrochemical industrial biological sludge. J. Hazard. Mater. 168(1): 438-444.

Xi H X, Li Z., Zhang H. B. (2003). Estimation of activated energy and isotherm of low-volatility dioxin by TPD technique. Sep. Purif. Technol. 31(1): 39-43.

Xue H B. (2011). Study on Adsorption and Desorption Behaviors of PAHs on Granular Activated

628 Carbon [Dissertation]. Nanjing: Nanjing University of Information Science & Technology,

629 Yang K U N, Wu W, Jing Q, et al. (2008).Aqueous adsorption of aniline, phenol, and their
630 substitutes by multi-walled carbon nanotubes. Environ. Sci. Technol. 42(21): 7931-7936.

631 Yang Q, Liu Y S, Li Z Y, et al (2015).Study on the adsorption behaviours of naphthalene on
632 MCM-41 and SBA-15 mesoporous molecular sieves. J. Fuel Chem. Technol. 43(12): 1482-
633 1488.

634 Yang X, Zhang C, Jiang L, et al(2019). Molecular Simulation of Naphthalene, Phenanthrene, and
635 Pyrene Adsorption on MCM-41. Int. J. Mol. Sci., 20(3): 665.

636 Yong G, Jin Z, Tong H, et al. (2006). Selective reduction of bulky polycyclic aromatic
637 hydrocarbons from mainstream smoke of cigarettes by mesoporous materials. Micropor.
638 Mesopor. Mat. 91(1-3): 238-243.

639 Yu L, Tu X, Li X, et al. (2010).Destruction of acenaphthene, fluorene, anthracene and pyrene by
640 a dc gliding arc plasma reactor. J. Hazard. Mater. 180(1-3): 449-455.

641 Zhang L, Li P, Gong Z, et al. (2008).Photocatalytic degradation of polycyclic aromatic
642 hydrocarbons on soil surfaces using TiO2 under UV light. J. Hazard. Mater. 158(2-3): 478-484.

643 Zhao D, Feng J, Huo Q, et al. (1998). Triblock copolymer syntheses of mesoporous silica with
644 periodic 50 to 300 angstrom pores. Science 279(5350): 548-552.

645 Zeng, W., & Bai, H. (2016). Adsorption/desorption behaviors of acetone over micro-/mesoporous
646 SBA-16 silicas prepared from rice husk agricultural waste. *Aerosol Air Qual. Res*, *16*, 2267-
647 2277.

648 Zhang, N., Cao, J., Li, L., Ho, S. S. H., Wang, Q., Zhu, C., & Wang, L. (2018). Characteristics
649 and source identification of polycyclic aromatic hydrocarbons and n-alkanes in $PM_{2.5}$ in
650 Xiamen. *Aerosol Air Qual. Res.*, 18: 1673–1683.

651 Zhong Z, Jin B, Huang Y, et al. (2008). Experimental study on flue gas purifying of MSW
652 incineration using in-pipe jet adsorption techniques. Waste Manage. 28(10): 1923-1932.

653 Zhou H C, Cai H X, Xue H B, et al. (2010a). Static adsorption mecha-nism of naphthalene on
654 carbonaceous sorbents. Res. Environ. Sci. 23(5):658-662.

655 Zhou H C, Zhong Z P, Jin B S, et al. (2005). Experimental study on the removal of PAHs using
656 in-duct activated carbon injection. Chemosphere 59(6): 861-869.

657 Zhou H C,Xie H B,Zhang C,et al. (2010b). Adsorption kinetics of naphthalene and acenaphthene
658 on activated carbon. Proc. CSEE 30 (32) :35-40

659 Zhou S L, Lü J, Xu H T, et al. (2008). The mechanism of micropore zeolites removing polycyclic
660 aromatic hydrocarbons in cigarette smoke. Acta Tabacaria Sinica 14(5): 1-6.

661 Zhou S L, Wang Y, Xu J H, et al. (2004). Removing polycyclic aromatic hydrocarbons and

662 nitrosamines in cigarette smoke by use of material with nano-porous structures. Jiangsu
663 Chemical Industry 32 (3) :29-31

664

665

666

667 **Table 1.** Characteristic of 16 USEPA priority PAHs.

Name of PAH	Abbr.	Molecular formula	F. W.	Boiling point(℃)	TEF[a,b]	Toxicity and preventive measures
naphthalene	NAP	$C_{10}H_8$	128	218	0.001	Low toxicity, irritating skin, mucous membranes, high concentration of inhalation can lead to anemia, liver and kidney damage, optic neuritis crystal opacity
acenaphthylene	ACY	$C_{12}H_8$	152	270	0.001	Avoid inhalation, skin contact with eyes
acenaphthene	ACE	$C_{12}H_{10}$	154	279	0.001	Micro-toxic, avoid inhalation, avoid contact with eyes and skin
fluorene	FLU	$C_{13}H_{10}$	166	294	0.001	avoid inhalation, avoid contact with eyes and skin
phenanthrene	PHE	$C_{14}H_{10}$	178	340	0.001	Irritating to the skin and carcinogenic effects
anthracene	ANT	$C_{14}H_{10}$	178	340	0.01	Mildly toxic, with mild local irritations and weak light perception
fluoranthene	FLT	$C_{16}H_{10}$	202	383	0.001	Micro-toxic, carcinogenic, corrosive, avoid inhalation and skin contact
pyrene	PYR	$C_{16}H_{10}$	202	404	0.001	Low toxicity, long-term exposure causes blood cell changes
1,2-benzanthracene	BaA	$C_{18}H_{12}$	228	435	0.1	Carcinogenic, inhaled skin contact is toxic, irreversible damage to the body
Chrysene	CHR	$C_{18}H_{12}$	228	448	0.01	Carcinogenic, inhaled or skin contact is toxic, irreversible damage to the body
benzo[b]fluoranthene	BbF	$C_{20}H_{12}$	252	481	0.1	Very carcinogenic
benzo[k]fluoranthene	BkF	$C_{20}H_{12}$	252	481	0.1	Very carcinogenic
benzo[a]pyrene	BaP	$C_{20}H_{12}$	252	496	1	The most toxic carcinogen in polycyclic aromatic hydrocarbons
indeno[1,2,3-c,d]pyrene	IcdP	$C_{22}H_{12}$	276	534	0.1	Less carcinogenic
dibenzo[a,h]anthracene	DahA	$C_{22}H_{14}$	278	535	1	Carcinogenic, avoid inhalation or contact with skin
benzo[g,h,i]perylene	BghiP	$C_{22}H_{12}$	276	542	0.01	Inhalation or skin contact is toxic, irreversible damage to the body

668 F.W. =Formula weight; [a] Liu et al,2017; [b] Jin et al., 2018

669 **Table 2.** Equilibrium adsorption capacities of PAH adsorbates on different adsorbents.

Adsorbates	Concentrations （mol m^{-3}）	Temperatures （℃）	adsorbents	Equilibrium adsorption capacities （mmol g^{-1}）	References
naphthalene	0.008	150	CA-3 （coke）	0.30	Mastral et al., 2001a
phenanthrene	0.012			0.52	
pyrene	0.007			0.53	
acenaphthene	0.013	150	RWE-1 （coke）	0.26	Mastral et al., 2003
fluorene	0.012			0.43	
anthracene	0.011			0.69	
phenanthrene	0.011			0.67	
naphthalene	0.016			1.00	
fluoranthene	0.010			0.64	
pyrene	0.010			0.69	
naphthalene	0.014	160	AC-1	2.81	Ma et al., 2004
fluorene	0.018			1.81	
phenanthrene	0.013			1.83	
naphthalene	0.005	140	AC-a	1.25	Zhou et al., 2010a
			AC-b	0.98	
			AC-c	1.72	
acenaphthene	0.014	150	CA-4 （tire）	0.29	Mastral et al., 2002a
			CA-15 （coal）	1.77	
			CA-16 （Apricot）	2.05	
			CA-5 （cherry）	0.03	
			CA-6(grape)	0.34	
			CA-11 （coconut）	1.77	
fluorene	0.012	150	CA-4	0.31	
			CA-12 （coal）	2.05	
			CA-16	2.29	
			CA-5	0.02	
			CA-6	0.60	
			CA-11	1.93	
phenanthrene	0.010	150	CA-4	0.65	
			CA-15	2.73	
			CA-16	3.34	
			CA-5	0.12	
			CA-6	0.75	
			CA-11	2.73	

anthracene	0.011	150	CA-4 CA-13 CA-16 CA-5 CA-6 CA-11	0.92 2.83 3.54 0.10 0.83 3.03	
naphthalene	0.006	120	OMC-B90 OMC-B50 OMC-B0 OMC-B10	0.51 1.21 1.48 1.76	Wang et al., 2012
phenanthrene	0.007	150	WSC WCSN2 WSCN10 WSCN30 WSCN60 WSCO15 WSCO30	2.13 1.89 1.83 1.75 1.75 2.01 2.10	Garcıa et al., 2004
naphthalene acenaphthene phenanthrene	0.005 0.002 0.002	140	AC-C_{max} AC-B_{max} AC-B_{max}	1.72 1.82 1.85	Cai, 2011
naphthalene acenaphthene phenanthrene	0.004 0.003 0.003	140	AC-2_{max} AC-1_{max} AC-1_{max}	1.45 1.58 1.40	Xue, 2011
phenanthrene	0.002	125	MCM-41 SBA-15 CMK-3	0.15 0.32 2.82	Li et al., 2017a
naphthalene	0.005	125	MCM-41 SBA-15 CMK-3	0.08 0.20 0.88	Yang et al., 2015
pyrene	0.0005	125	MCM-41 SBA-15 CMK-3	0.18 0.74 2.35	Li et al., 2017b
naphthalene	0.0005 0.0005	125	CMK-5 FDU-15	1.22 0.97	Meng et al., 2017

670

671

672 **Table 3.** Adsorption kinetics parameters of PAHs on mesoporous adsorbents.

Adsorbents	PAHs	C_0 (mmol m^{-3})	$k_L a$ (s^{-1})	$k_f a$ (s^{-1})	k_P (s^{-1})	References
ICB5		1.79×10^{-5}	-	-	1.0×10^{-3}	
ICB5		4.33×10^{-5}	-	-	1.5×10^{-3}	
ICB5		1.12×10^{-4}	-	-	2.0×10^{-3}	
ICB5		6.25×10^{-4}	-	-	2.5×10^{-3}	
ICB5		2.68×10^{-3}	-	-	4.0×10^{-3}	
ICB8		6.70×10^{-5}	-	-	1.0×10^{-3}	
ICB8	phenanthrene	3.13×10^{-4}	-	-	2.0×10^{-3}	Murillo et al., 2004
ICB8		1.25×10^{-3}	-	-	3.0×10^{-3}	
ICB8		3.30×10^{-3}	-	-	5.0×10^{-3}	
ICB12		8.04×10^{-5}	-	-	1.0×10^{-3}	
ICB12		2.86×10^{-4}	-	-	2.0×10^{-3}	
ICB12		1.65×10^{-3}	-	-	3.5×10^{-3}	
ICB12		3.79×10^{-3}	-	-	4.5×10^{-3}	
SBA-15	naphthalene	0.143	2.72	7.2×10^{3}	5.0×10^{-3}	Liu et ;al., 2016
		0.949	3.13	7.2×10^{3}	2.6×10^{-3}	
		2.76	9.71	7.2×10^{3}	8.9×10^{-4}	
SBA-15	phenanthrene	0.097	6.51	6.3×10^{3}	1.5×10^{-3}	Li et al., 2017a
		0.41	7.08	6.3×10^{3}	1.8×10^{-3}	
		2.2	15.51	6.3×10^{3}	3.7×10^{-3}	
SBA-15	pyrene	0.29	20.27	5.0×10^{3}	5.2×10^{-4}	Meng et al., 2017
		0.46	22.93	5.0×10^{3}	1.3×10^{-3}	
		0.71	53.49	5.0×10^{3}	2.9×10^{-3}	
MCM-41	naphthalene	0.143	1.61	4.9×10^{3}	3.5×10^{-3}	Liu et al., 2016
		0.949	2.52	4.9×10^{3}	17×10^{-3}	
		2.76	7.43	4.9×10^{3}	7.5×10^{-3}	
MCM-41	phenanthrene	0.097	6.02	6.5×10^{3}	2.9×10^{-3}	Li et al., 2017a
		0.41	7.53	6.5×10^{3}	3.6×10^{-3}	
		2.2	9.63	6.5×10^{3}	4.2×10^{-3}	
MCM-41	pyrene	0.29	23.47	5.4×10^{3}	1.5×10^{-3}	Meng et al., 2017
		0.46	9.98	5.4×10^{3}	9.8×10^{-4}	
		0.71	12.16	5.4×10^{3}	1.0×10^{-3}	
CMK-3	naphthalene	0.143	73.4	1.6×10^{4}	7.5×10^{-3}	Liu et al., 2016
		0.949	5.5	1.6×10^{4}	8.9×10^{-4}	
		2.76	30.6	1.6×10^{4}	7.9×10^{-3}	
CMK-3	phenanthrene	0.097	6.43	1.4×10^{4}	4.1×10^{-4}	Li et al., 2017a
		0.41	7.7	1.4×10^{4}	9.7×10^{-4}	
		2.2	9.87	1.4×10^{4}	1.1×10^{-3}	
CMK-3	pyrene	0.29	51.86	1.4×10^{4}	2.8×10^{-3}	Meng et al., 2017
		0.46	36.71	1.4×10^{4}	2.2×10^{-3}	
		0.71	14.62	1.4×10^{4}	9.9×10^{-4}	

673

674

675 **Table 4.** Parameters of PAHs thermal desorption on various sorbents

Adsorbents	Adsorbate	TPD peak temperature（K）	desorption activation energy（kJ mol^{-1}）	References
MCM-41	phenanthrene	452～472	68.7	Li et al., 2017a
SBA-15		452～464	116.2	
CMK-3		482～496	127.0	
AC_{WY}	naphthalene	505～534	65.14	Li et al., 2015
	acenaphthene	569～599	83.81	
AC_{NT}	naphthalene	515～535	101.40	
	acenaphthene	613～636	124.91	
MCM-41	naphthalene	384～400	73.55	Li et al., 2016
SBA-15		369～387	59.76	
CMK-3		422～441	77.92	
MCM-41	pyrene	494～509	129.04	
SBA-15		480～512	54.87	
CMK-3		514～538	87.03	
CMK-5	naphthalene	395～409	57.23	Meng et al., 2017
FDU-15		428～434	47.09	
AC	naphthalene	535～575	65.89	Xue, 2011
	acenaphthene	617～637	96.13	
	phenanthrene	690～719	105.62	
	fluoranthene	743～779	128.03	
AC	naphthalene	535～575	65.89	Zhou et al., 2010b
	acenaphthene	617～638	96.13	

676

677

678

679 **Figure Captions**

680 **Fig. 1.** Chemical structures of the 16 USEPA priority PAH compounds.

681 **Fig. 2.** Structure diagrams of MCM-41, SBA-15 and CMK-3 for PAHs adsorption.

682 **Fig. 3.** Phenanthrene adsorption isotherms on a carbonaceous material (CA-3 sample) at different

683 CO_2 concentrations (T= 150 °C, $0.02 < C_0 < 3$ ppmv)

684

685

686

687

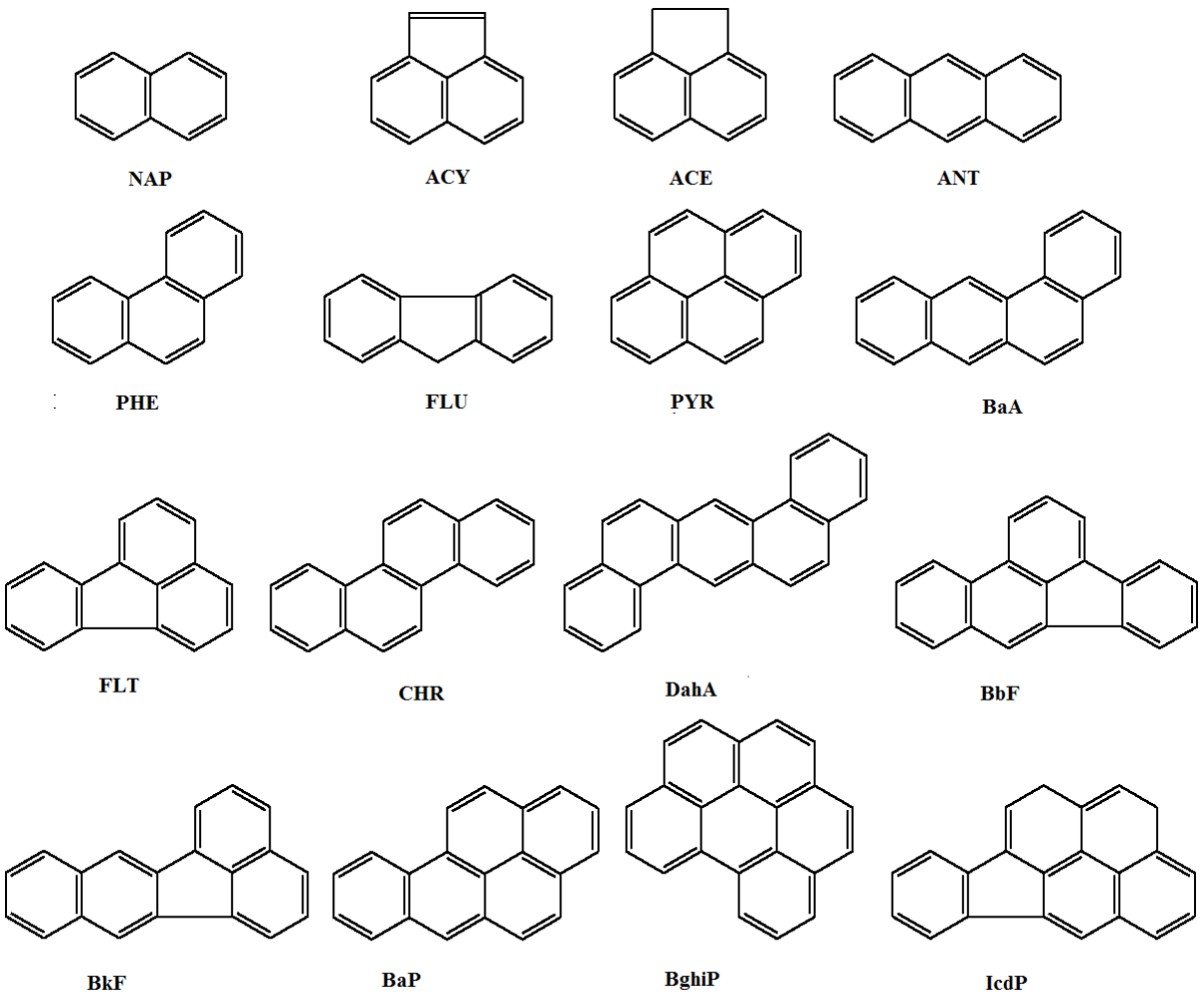

688

689

690

691

692

693 **Fig. 1.**

694

Fig. 2.

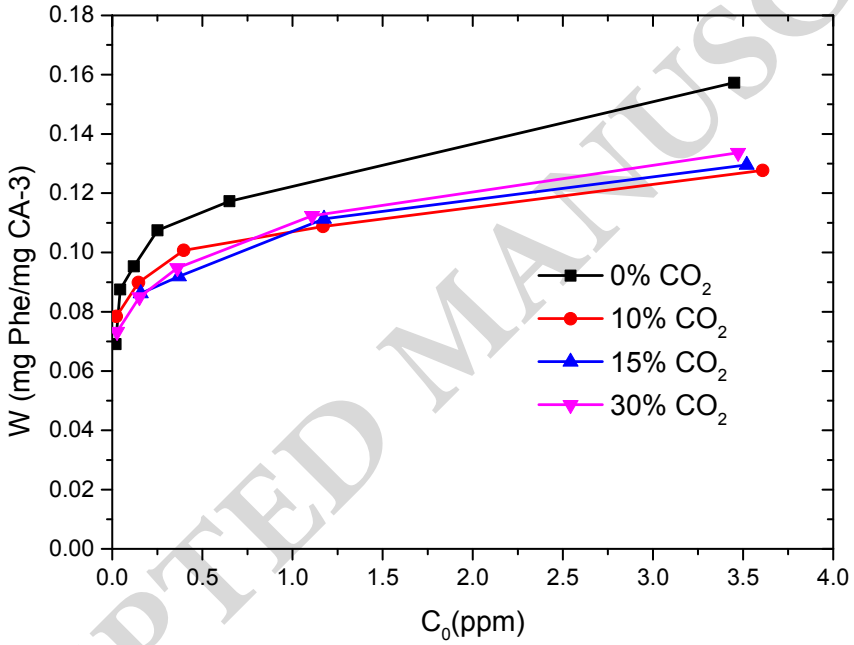

Fig. 3.